Knudsen Corrections for the Senftleben-Beenakker Effect of Viscosity

H. Vestner

Institut für Theoretische Physik der Universität Erlangen-Nürnberg, Erlangen

(Z. Naturforsch. **29 a**, 663—677 [1974]; received October 18, 1973)

A rarefied polyatomic gas between infinite parallel plates which is subject to a pressure gradient and to a magnetic field is considered. The tensor polarization and the Kagan polarization account for the influence of the field on the gas flow. In the slip flow regime differential equations and boundary conditions for the velocity and the tensor polarization are solved. The dependence of the solution on the mean pressure and on the magnetic field is discussed. Knudsen corrections for the Senftleben-Beenakker effect of viscosity are derived. By comparison with experimental data of Hulsman et al. a set of surface parameters is obtained. They characterize mechanical slip, thermomagnetic slip, and the influence of gas-wall collisions on the tensor polarization.

The influence of a magnetic field on transport phenomena in polyatomic gases, often referred to as Senftleben-Beenakker effect (SBE), has been studied intensively in the last decade, both experimentally and theoretically [1]. A magnetic field can act on flow and heat conduction via polarizations set up by collisions in a nonequilibrium situation. The analysis of experimental data reveals that the most important types of alignments in a streaming or a heat conducting nonpolar gas are the tensor polarization [2–4] and the tensor polarization flux (often called Kagan polarization) [5], respectively. These polarizations are nonequilibrium averages of second and third rank tensors built up from the rotational angular momentum and the velocity of a molecule.

In the hydrodynamic regime the SBE depends on the field strength H and on the mean pressure p_0 only in the combination H/p_0 which is essentially the ratio of the precession frequency and a collision frequency [1]. But at lower pressures, i. e. when the mean free path of a molecule becomes comparable with the dimensions of a macroscopic container, deviations from this simple H/p_0 dependence have been observed [2–5]. Then an additional pressure dependence occurs which is due to slip effects for the velocity and to the influence of gas-wall collisions on the tensor polarization. For example, the maximum value of the transverse effects (i. e. η_4, η_5, $\lambda_{\mathrm{trans}\,v}$) decreases with decreasing pressure and the position of this reduced maximum is shifted to higher H/p_0 values [3]. The method for a calculation of these Knudsen corrections [6] is worked out in detail in the present paper for the SBE of viscosity. A short summary of the results has already been presented in Reference [7].

The theoretical basis for a treatment of alignment phenomena in polyatomic gases is the quantum mechanical kinetic equation due to Waldmann and Snider [8]. By the application of a Chapman-Enskog approach [9] or of the moment method [10] differential equations and constitutive laws for macroscopic variables have been derived from the Waldmann-Snider equation. Relevant for the SBE of viscosity is the coupling of the tensor polarization with the friction pressure tensor. In the hydrodynamic regime the tensor polarization is proportional to the velocity gradient, thus expressions for the five viscosity coefficients are obtained [9, 11]. But in the slip flow regime the tensor polarization flux cannot be neglected for the treatment of a streaming gas [6, 7]. Then the moment method supplies us with a differential equation for the tensor polarization [6, 7, 12] which has to be solved besides the Navier-Stokes equation. By the way, the differential equation for the velocity is modified [6, 7, 12] due to the existence of the polarizations. Consequently, also boundary conditions for the velocity and the tensor polarization have to be used now. Phenomenological boundary conditions for macroscopic variables have been derived by Waldmann's thermodynamic method [13] from the entropy production at the interface between the gas and a solid body [6, 7, 12].

In this paper a rarefied polyatomic gas between infinite parallel plates is considered. This serves as a simple theoretical model for the flat rectangular

Reprint requests to Dr. H. Vestner, Institut für Theoretische Physik der Universität Erlangen-Nürnberg, *D-8520 Erlangen*, Glückstraße 6.

Dieses Werk wurde im Jahr 2013 vom Verlag Zeitschrift für Naturforschung in Zusammenarbeit mit der Max-Planck-Gesellschaft zur Förderung der Wissenschaften e.V. digitalisiert und unter folgender Lizenz veröffentlicht: Creative Commons Namensnennung-Keine Bearbeitung 3.0 Deutschland Lizenz.

This work has been digitalized and published in 2013 by Verlag Zeitschrift für Naturforschung in cooperation with the Max Planck Society for the Advancement of Science under a Creative Commons Attribution-NoDerivs 3.0 Germany License.

Zum 01.01.2015 ist eine Anpassung der Lizenzbedingungen (Entfall der Creative Commons Lizenzbedingung „Keine Bearbeitung") beabsichtigt, um eine Nachnutzung auch im Rahmen zukünftiger wissenschaftlicher Nutzungsformen zu ermöglichen.

On 01.01.2015 it is planned to change the License Conditions (the removal of the Creative Commons License condition "no derivative works"). This is to allow reuse in the area of future scientific usage.

capillary used by Hulsman et al.[3,4] for a measurement of the viscosity coefficients. The gas is subject to a pressure gradient. Furthermore, the whole system is placed in a magnetic field and is part of a gas-flow Wheatstone bridge.

In Section 1 differential equations and boundary conditions for the tensor polarization and the velocity are solved by a perturbation method. The same set of equations has recently been used for a calculation of Knudsen corrections for flow birefringence in gases[14]. In both cases the value of the tensor polarization at the wall is determined by gas-wall collisions, whereas its value far away from the walls is established by gas-gas collisions. The transition between these two values occurs in a small boundary layer where both types of collisions are important.

The dependence of the flow velocity and the pressure gradients on the mean pressure and on the magnetic field is discussed in detail in Section 2. Here only terms up to first order in the mean free path are taken into account. In the bulk of the gas (i. e. far away from the plates) the velocity profile is nearly parabolic. But in the boundary layer near the walls oscillations occur due to the exponential terms which trace back to the spatial dependence of the tensor polarization.

Finally, in Section 3, the Knudsen corrections for the pressure gradients are compared with experimental data obtained by Hulsman et al.[3,4] for the SBE of viscosity. Numerical values for the relevant surface parameters are derived.

I. Solution of Differential Equations and Boundary Conditions

For a measurement of all five viscosity coefficients a flat rectangular capillary of length D_z, width D_x and thickness D_y was used[3,4]. Since the inequality

$$D_z \gg D_x \gg D_y$$

applies the flow of a polyatomic gas between infinite parallel plates of distance $D_y = 2\,\mathrm{d}$ is treated here instead of that in the real set up. The unit vector in y-direction, perpendicular to the plates, is denoted by $\boldsymbol{u}$; the plates are placed at $y = \pm d$.

In the absence of a magnetic field a constant pressure gradient

$$\nabla p^{(0)} = \boldsymbol{e}\,(\mathrm{d}p/\mathrm{d}z_0 \tag{1.1}$$

shall be applied, $\boldsymbol{e}$ is a unit vector in z-direction parallel to the plates. If a magnetic field $\boldsymbol{H} = H\,\boldsymbol{h}$ $(\boldsymbol{h}\cdot\boldsymbol{h} = 1)$ is present additional pressure gradients $\nabla p^{(1)}$ occur

$$\nabla p = \nabla p^{(0)} + \nabla p^{(1)}, \quad \nabla p^{(1)} = \boldsymbol{0} \text{ for } H = 0\,. \tag{1.2}$$

The major aim is the determination of the x- and z-components of $\nabla p^{(1)}$. For this purpose the flow pattern has to be calculated.

The influence of a magnetic field on the flow of a polyatomic gas is due to the mutual coupling between the friction pressure tensor and alignments set up by collisions. The most important type is the (second rank) tensor polarisation $\mathbf{a}$[2–4]. Furthermore, in a rarefied gas, the (third rank) tensor polarization flux (Kagan polarization) $\underline{\mathbf{b}}$[5] cannot be neglected[6,7]. Experimental results for the SBE show[1] that the field induced change of viscosity is for all diamagnetic gases less than one percent. Thus the following perturbation method can be used.

The flow velocity

$$\boldsymbol{v}(y, \boldsymbol{H}) = \boldsymbol{v}_{\text{iso}}(y) + \boldsymbol{v}_1(y, \boldsymbol{H}) \tag{1.3}$$

is split up into two parts. For a calculation of the "isotropic" velocity $\boldsymbol{v}_{\text{iso}}(y)$ the polarizations $\mathbf{a}$ and $\underline{\mathbf{b}}$ are neglected. Then the tensor polarization and its flux are determined from $\boldsymbol{v}_{\text{iso}}(y)$ and $\nabla p^{(0)}$. Finally, the field dependent quantities $\nabla p^{(1)}$ and $\boldsymbol{v}_1(y, \boldsymbol{H})$ are calculated from these anisotropic alignments. If $\mathbf{a}$ and $\underline{\mathbf{b}}$ are both put equal to zero, $\nabla p^{(1)}$ and $\boldsymbol{v}_1(y, \boldsymbol{H})$ vanish. For $H = 0$ the anisotropic velocity

$$\boldsymbol{v}_1(y, \boldsymbol{H}) = \boldsymbol{v}^0(y) + \boldsymbol{v}^H(y), \quad \boldsymbol{v}_1(y, \boldsymbol{0}) = \boldsymbol{v}^0(y) \tag{1.4}$$

does not vanish, it reduces to $\boldsymbol{v}^0(y)$. Hence, $\boldsymbol{v}^H(y)$ is the field dependent part of the total velocity, with $\boldsymbol{v}^H(y) = \boldsymbol{0}$ for $H = 0$.

This perturbation method is applied here to constitutive laws, differential equations and boundary conditions derived in Refs.[6,12] from moments equations of the Waldmann-Snider equation[8].

(a) Isotropic Flow Velocity

In isotropic approximation temperatures T and T' (the difference between translational and rotational temperature[6,12]) are constant

$$T_{\text{iso}} = \text{constant} = T_0\,, \quad T'_{\text{iso}} = 0\,. \tag{1.5}$$

Consequently the heat fluxes are determined by the constant pressure gradient only, e. g. the translational heat flux is given by [6, 12]

$$(\boldsymbol{q}_{\text{trans}})_{\text{iso}} = \frac{2}{5} \frac{T_0}{p_0} \lambda_{\text{iso}}^{\text{t}} \nabla p^{(0)} . \qquad (1.6)$$

Then we have for the friction pressure tensor

$$\overline{\mathsf{p}}_{\text{iso}} = -2\,\eta_{\text{iso}} \overline{\nabla \boldsymbol{v}}_{\text{iso}} . \qquad (1.7)$$

The isotropic flow velocity is calculated from the differential equations

$$\nabla \cdot \boldsymbol{v}_{\text{iso}} = 0 , \quad \frac{1}{\eta_{\text{iso}}} \nabla p^{(0)} - \nabla \cdot \nabla \boldsymbol{v}_{\text{iso}} = \boldsymbol{0}$$

and from the normal and tangential boundary conditions [6, 7, 12]

$$\boldsymbol{v}_{\text{iso}} \cdot \boldsymbol{n} = 0 , \quad (\boldsymbol{v} + \tfrac{2}{5} p_0^{-1} \boldsymbol{q}_{\text{trans}})_{\text{iso}}^{\tan} = \frac{l}{\eta_{\text{iso}}} C_{\text{m}} \boldsymbol{k}_{\text{iso}}^{\tan} .$$

Here, $\boldsymbol{n}$ denotes the outer unit normal of the gas, i.e. $\boldsymbol{n} = \pm \boldsymbol{u}$ for $y = \pm d$. If $\boldsymbol{v}_{\text{iso}}$ has only a z-component and depends on y then $\nabla \cdot \boldsymbol{v}_{\text{iso}} = 0$ and $\boldsymbol{v}_{\text{iso}} \cdot \boldsymbol{n} = 0$ are fulfilled identically. With $\boldsymbol{k}_{\text{iso}}^{\tan} = (\overline{\mathsf{p}}_{\text{iso}} \cdot \boldsymbol{n})^{\tan}$ and $(\boldsymbol{q}_{\text{trans}})_{\text{iso}}$ from Eq. (1.6) the well-known parabolic velocity profile for the plane Poiseuille flow is obtained:

$$\boldsymbol{v}_{\text{iso}}(y) = -\frac{d^2}{2\,\eta_{\text{iso}}} \nabla p^{(0)} \cdot \left[1 - \left(\frac{y}{d}\right)^2 + 2 \frac{l}{d} C_{\text{m}} + \frac{4}{5} \frac{l_\eta l_{\text{t}}}{d^2} \right] . \qquad (1.7)$$

For nonzero Knudsen number l/d the mean velocity

$$\overline{\boldsymbol{v}}_{\text{iso}} \equiv \frac{1}{2d} \int_{-d}^{+d} \mathrm{d}y\, \boldsymbol{v}_{\text{iso}}(y) = -\frac{d^2}{3\,\eta_{\text{iso}}} \nabla p^{(0)} \left[1 + 3 \frac{l}{d} C_{\text{m}} + \frac{6}{5} \frac{l_\eta l_{\text{t}}}{d^2} \right] \qquad (1.8)$$

is enlarged by mechanical ($\propto l\, C_{\text{m}}$) and by thermal slip ($\propto l_\eta l_{\text{t}}$). The lengths l, l_η, l_{t} occurring in Eqs. (1.7), (1.8) are mean free paths defined by

$$l = \frac{8}{5} \sqrt{\frac{2}{\pi}}\, l_\eta ,$$

$$l_\eta = \frac{c_0}{\sqrt{3}\, \omega_\eta} , \quad l_{\text{t}} = \frac{c_0}{\sqrt{3}\, \omega_{\text{t}} (1 - A_{\text{tr}})} , \qquad (1.9)$$

where $c_0 = \sqrt{3\,k T_0 / M}$, M is the mass of a molecule and k is Boltzmann's constant. The relaxation constants ω_η and ω_{t} are related to the isotropic viscosity $\eta_{\text{iso}} = p_0/\omega_\eta$ and to the heat conductivity coefficient

$$\lambda_{\text{iso}}^{t} = \frac{5}{2} \frac{k}{M} \frac{p_0}{\omega_{\text{t}} (1 - A_{\text{tr}})} .$$

The coupling between the translational and the rotational heat fluxes is characterized by [12]

$$A_{\text{tr}} = \omega_{\text{tr}}^2 / \omega_{\text{t}}\, \omega_{\text{r}} .$$

(b) *Tensor Polarization and Kagan Polarization*

By use of the isotropic solutions (1.5), (1.6), (1.7) the following differential equations

$$(1 - L_{\text{m}}^2 \nabla \cdot \nabla)\, \mathsf{P}^{(m)} : \mathbf{a} = \frac{\sqrt{2}\, \omega_{\eta \text{T}}}{\omega_\eta\, \omega_{\text{T}}} \frac{1}{1 + i\, m\, \varphi_{\text{T}}} \mathsf{P}^{(m)} : \overline{\nabla \boldsymbol{v}}_{\text{iso}} , \quad m = 0, \pm 1, \pm 2 ,$$

and boundary conditions for the tensor polarization

$$\mathbf{a} = \sum_{m=-2}^{+2} \mathsf{P}^{(m)} : \mathbf{a} = C_{\text{am}}\, p_0^{-1} \overline{\boldsymbol{k}_{\text{iso}}^{\tan} \boldsymbol{n}} + C_{\text{a}}\, \boldsymbol{n} \cdot \mathbf{b} \qquad (\text{for } y = \pm d)$$

are obtained [6, 7, 12].

The dimensionless coefficients C_{a} and C_{am} characterize the destruction and production of tensor polarization by gas-wall collisions [7]. The positive surface parameter C_{a} is some sort of accommodation coefficient for the tensor polarization [15], hence it is expected to be of order 1. In contradistinction, the non-diagonal coefficient C_{am} (which can have both signs) is expected to be small compared to 1 (e.g. of order $\omega_{\eta\text{T}}/\omega_{\text{T}}$) since it describes a production mechanism for tensor polarization by gas-wall collisions. Recently, Halbritter [15] has related C_{am} to the "noncentral" part of the interaction potential between the gas molecule and the wall.

The Kagan polarization is calculated from [12]

$$b_{\lambda,\mu\nu} = \sum_{m=-2}^{+2} \mathsf{P}^{(m)}_{\mu\nu,\mu'\nu'} \frac{1}{1 + i\, m\, \varphi_b} \left[-l_b \frac{\partial a_{\mu'\nu'}}{\partial x_\lambda} + (a_{\lambda'}^{\text{rt}})_{\text{iso}}\, \Delta_{\lambda'\lambda,\mu'\nu'} \right]$$

with
$$\boldsymbol{a}_{\text{iso}}^{\text{rt}} = -\frac{\sqrt{2}\,\omega_{\eta\text{T}}}{\omega_\text{T}}\frac{l_b}{p_0}\,a_{\text{Tt}}\nabla p^{(0)}\,.$$

Here, the abbreviations

$$L_\text{m} = \frac{c_0}{\sqrt{3}\,\omega_\text{T}\,\omega_\text{b}}\left[(1+i\,m\,\varphi_\text{b})(1+i\,m\,\varphi_\text{T})\right]^{-1/2},\quad l_b = \frac{c_0}{\sqrt{3}\,\omega_b},\quad a_{\text{Tt}} = \frac{1}{5}\frac{\omega_\text{T}}{\omega_\text{t}}\left(1-\frac{\omega_{\text{tr}}\,\omega_{\text{br}}}{\omega_{bt}\,\omega_\text{r}}\right)(1-A_{\text{tr}})^{-1}$$

have been used. The field strength H is contained in the precession angles

$$\varphi_\text{T} = \omega_H/\omega_\text{T}\,,\quad \varphi_b = \omega_H/\omega_b\,.$$

Since $\omega_H = \gamma H$ (γ is the rotational gyromagnetic ratio) and $\omega_\text{T}, \omega_\text{b} \propto p_0$ apply we have $\varphi_\text{T}, \varphi_\text{b} \propto H/p_0$. The field direction $\boldsymbol{h}$ enters via the fourth rank projection tensors $\mathcal{P}^{(m)}$ introduced by Hess [16, 11].

The ansatz

$$\mathbf{a} = \frac{\sqrt{2}\,\omega_{\eta\text{T}}}{\omega_\text{T}}\frac{d}{p_0}\left(\frac{\text{d}p}{\text{d}z}\right)_0 \sum_{m=-2}^{+2} A_\text{m}(y)\,\mathcal{P}^{(m)} : \overline{\boldsymbol{e}\,\boldsymbol{u}} \tag{1.10}$$

yields then the solution

$$A_\text{m}(y) = \frac{y}{d}\frac{1}{1+i\,m\,\varphi_\text{T}} - a_m\frac{\sinh y/L_\text{m}}{\sinh d/L_\text{m}}\,, \tag{1.11}$$

with

$$a_\text{m} = \left[\frac{1}{1+i\,m\,\varphi_\text{T}} + \tilde{C}_{\text{am}} + \tilde{C}_\text{a}\frac{L_0}{\text{d}}\frac{1}{1+i\,m\,\varphi_\text{b}}\left(\frac{1}{1+i\,m\,\varphi_\text{T}} + a_{\text{Tt}}\right)\right]\left[1+\tilde{C}_\text{a}\sqrt{\frac{1+i\,m\,\varphi_\text{T}}{1+i\,m\,\varphi_\text{b}}}\coth\frac{d}{L_\text{m}}\right]^{-1}.$$

For convenience, the coefficients $\tilde{C}_\text{a}$, $\tilde{C}_{\text{am}}$ have been introduced:

$$C_\text{a} = \sqrt{\omega_b/\omega_\text{T}}\,\tilde{C}_\text{a}\,,\quad C_{\text{am}} = \tilde{C}_{\text{am}}\sqrt{2}\,\omega_{\eta\text{T}}/\omega_\text{T}\,.$$

The second contribution to $A_m(y)$ describes the influence of gas-wall collisions on the tensor polarization. For $L_0/d \ll 1$ it is only important near the boundary (at $y = \pm d$) within a small layer of thickness of a few mean free paths L_0. Within the gas (i. e. outside this boundary layer) the tensor polarization assumes a value

$$A_\text{m}^\infty(y) = \frac{y}{d}\frac{1}{1+i\,m\,\varphi_\text{T}} \tag{1.12}$$

which is determined by gas-gas collisions only. The transition from the boundary value

$$A_\text{m}(\pm d) = \pm\left(\frac{1}{1+i\,m\,\varphi_\text{T}} - a_\text{m}\right) \tag{1.13}$$

to $A_\text{m}^\infty(y)$ occurs within this boundary layer. For infinite pressure p_0 (i. e. $L_0/d = 0$) there is a sudden jump from the boundary value

$$(A_\text{m}^\infty)_{\pm d} \equiv \pm\left(\frac{1}{1+i\,m\,\varphi_\text{T}} - a_m\right)_{L_0=0}$$

to $A_\text{m}(y) = A_\text{m}^\infty(y)$ for $-d<y<d$.

For $H=0$ this boundary value

$$(A_0^\infty)_d = (\tilde{C}_\text{a} - \tilde{C}_{\text{am}})/(\tilde{C}_\text{a}+1)$$

is greater than $A_0^\infty(y\to+d)=1$, if $-\tilde{C}_{\text{am}}>1$ applies. Then there is a net production of tensor polarization by gas-wall collisions, and this production increases with increasing $\tilde{C}_\text{a}>0$. For $-\tilde{C}_{\text{am}}<1$ the inequality

$$(A_0^\infty)_d < A_0^\infty(y\to+d) = 1$$

is valid, and the difference between both values decreases with increasing $\tilde{C}_\text{a}$.

In Fig. 1, for $H=0$, the spatial dependence of the tensor polarization in HD is shown for different values of L_0/d. For the calculation of $A_0(y)$ from Eq. (1.11) the parameters from Table 2 and Table 3 are used.

If the magnetic field is perpendicular to the plates, $\boldsymbol{h}=\boldsymbol{u}$, the tensor polarization has only two nonzero components (see Appendix A):

$$\boldsymbol{h}=\boldsymbol{u},\ \mathbf{a} = \frac{\sqrt{2}\,\omega_{\eta\text{T}}}{\omega_\text{T}}\frac{d}{p_0}\left(\frac{dp}{dz}\right)_0 \cdot\left[A_1'\,\overline{\boldsymbol{u}\,\boldsymbol{e}} + A_1''\,\overline{\boldsymbol{u}\,\boldsymbol{u}\times\boldsymbol{e}}\right]. \tag{1.14}$$

The functions A_1' and A_1'' are the real and imaginary parts of A_1. Their spatial dependence is shown

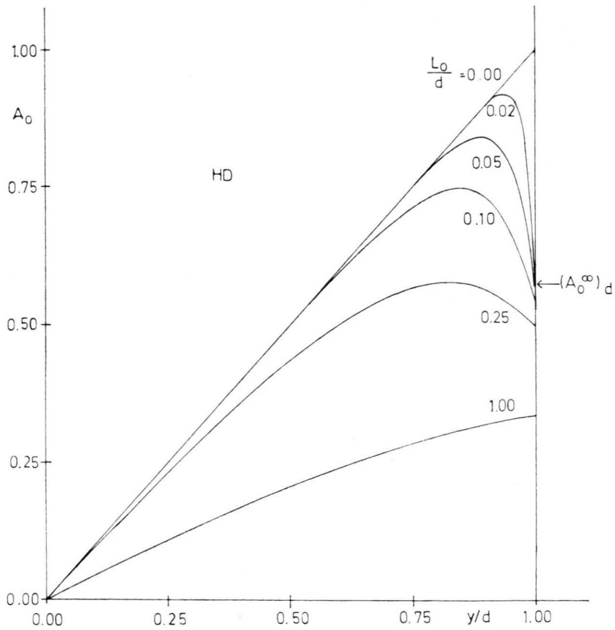

Fig. 1. Spatial dependence of tensor polarization **a** at $H=0$ in HD for some values of L_0/d, $\mathbf{a} \propto A_0(y) \overline{\boldsymbol{u}\,\boldsymbol{e}}$. The function $A_0(y)$ is calculated from Eq. (1.11) with the parameters of Table 2, Table 3. The boundary value of A_0 for infinite pressure is indicated by $(A_0^\infty)_\mathrm{d}$. The A's are odd functions of y/d.

Table 1. Experimentally observed Knudsen parameters for the SBE of viscosity [3, 4].

	n_α [3, 4]	n_β^{long} [4]	n_γ^{long} [4]	n_β^{tr} [3]	n_γ^{tr} [3]
HD	6	6	14	10	12
CH_4	6	9	3	10	3
CO	6	10	2	10	2
N_2	6	12	4	10	2

Table 2. Numerical values for some quantities which are relevant for the SBE of viscosity [2–4], see also Reference [12]. Measurements of flow birefringence [18] show that $\omega_{\eta T}$ is positive for HD, CO, N_2. For a calculation of a_{Tt} the signs of ω_{br} and ω_{bt} have been assumed to be equal. The mean free path l [see (1.9)] has been calculated for $p_0 = 1$ Torr, $T_0 = 293$ K with the viscosity data used in Reference [12].

	$A_{\eta\mathrm{T}} \cdot 10^3$	$\sqrt{2}\,\dfrac{\lvert\omega_{\eta\mathrm{T}}\rvert}{\omega_\mathrm{T}}$	a_{Tt}	$\varkappa = \dfrac{\omega_\mathrm{T}}{\omega_\tau}$	L_0/l	l mm
HD	1.88	0.175	0.04	0.16	2.68	0.091
CH_4	0.83	0.047	0.30	0.56	0.78	0.041
CO	3.64	0.091	0.40	0.64	0.71	0.049
N_2	2.73	0.092	0.32	0.47	0.85	0.050

Table 3. Theoretical Knudsen parameters for the SBE of viscosity. The correction factors N_S, n_S, N_M, n_M have been calculated from Equations (2.14) – (2.17). They should be compared with the experimental values [3, 4] for $\frac{1}{2} n_\beta^{\mathrm{long}}$, $\frac{1}{2} n_\gamma^{\mathrm{long}}$, $\frac{1}{2} n_\beta^{\mathrm{tr}}$, $\frac{1}{2} n_\gamma^{\mathrm{tr}}$ given in Table 1.

	C_m	$\tilde{C}_\mathrm{a}$	$\tilde{C}_\mathrm{ma}$	C_a	C_ma	N_S	n_S	N_M	n_M
HD	1.0	0.4	0.4	1.00	0.07	3.5	6.5	4.9	5.5
CH_4	1.0	0.6	0.0	0.80	0.00	4.5	1.3	4.6	1.3
CO	1.2	1.1	0.0	1.38	0.00	4.7	1.0	4.7	1.0
N_2	1.2	1.0	0.0	1.46	0.00	4.9	1.2	5.0	1.1

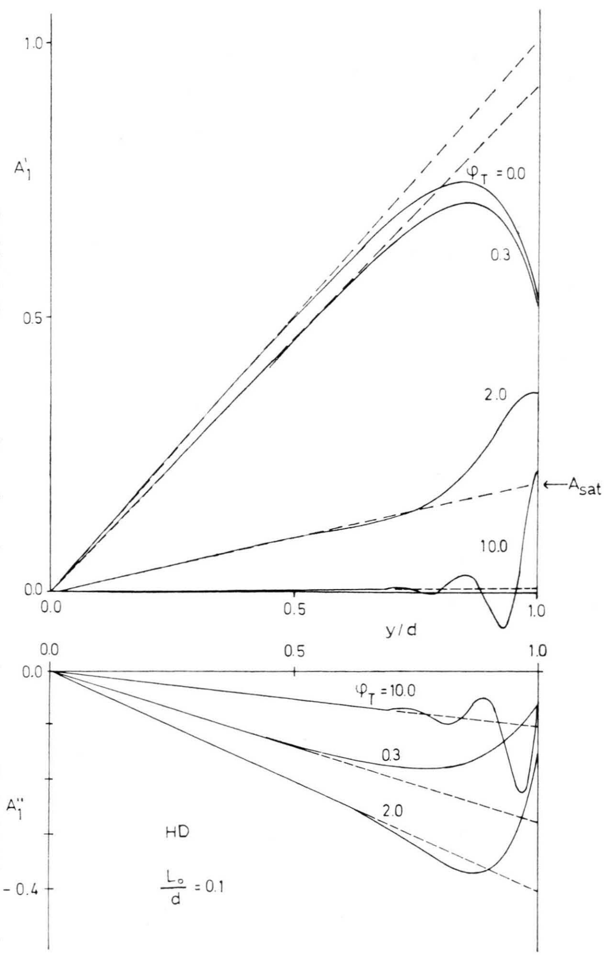

Fig. 2. Spatial dependence of tensor polarization **a** in HD for $L_0/d = 0.1$, $\overline{\boldsymbol{h} = \boldsymbol{u}}$, and $\varphi_\mathrm{T} = 0.0$, 0.3, 2.0, 10.0; $\mathbf{a} \propto A_1' \overline{\boldsymbol{u}\,\boldsymbol{e}} + A_1'' \overline{\boldsymbol{u}\,\boldsymbol{u} \times \boldsymbol{e}}$, see Eq. (1.14). The dotted straight lines refer to $L_0/d = 0$. The boundary value for high magnetic field is indicated by A_sat, cf. Equation (1.15). For A_1', A_1'' see Eq. (1.11) and Table 2, Table 3. The A's are odd functions of y/d.

in Fig. 2 for HD, $L_0/d = 0.1$, and some values of φ_T. By the way, for $\varphi_T = 10$ the molecule performs about one precession during its free flight over a mean free path L_0. For high magnetic field ($|\varphi_T| \gg 1$) only the tensor polarization near the wall survives:

$$A_1'(\pm d)|_{\varphi_T\to\infty} \equiv \pm A_{sat} \approx \frac{-\tilde{C}_{am}}{1+\tilde{C}_a\sqrt{\omega_b/\omega_T}},$$

$$A_1''(\pm d)|_{\varphi_T\to\infty} \approx 0, \quad \text{i.e.} \tag{1.15}$$

$$\mathbf{a}(\pm d) \approx \mp \frac{d}{p_0}\left(\frac{dp}{dz}\right)_0 \frac{C_{am}}{1+C_a}\overline{\boldsymbol{u}\boldsymbol{e}}$$

$$\text{for } H\to\infty \text{ and } \boldsymbol{h} = \boldsymbol{u}.$$

Notice that the coefficient C_{am} characterizes a production mechanism for the tensor polarization at the wall.

(c) Anisotropic Flow Velocity and Field Dependent Pressure Gradient

The anisotropic velocity $\boldsymbol{v}_1(y,\boldsymbol{H})$ is determined by the polarizations $\mathbf{a}$ and $\underline{\mathbf{b}}$. From the continuity equation $\nabla\cdot\boldsymbol{v}_1 = 0$ and from the normal boundary condition $\boldsymbol{n}\cdot\boldsymbol{v}_1(\pm d,\boldsymbol{H}) = 0$ we easily derive that $\boldsymbol{v}_1$ has only tangential components, i. e.

$$\boldsymbol{u}\cdot\boldsymbol{v}_1(y,\boldsymbol{H}) \equiv 0. \tag{1.16}$$

Due to the existence of the tensor polarization and its flux the temperatures in the rarefied gas are no longer constant,

$$T = T_0 + T_1(y,\boldsymbol{H}), \quad T' = T_1'(y,\boldsymbol{H}).$$

But T_1 and T_1' are not needed for a calculation of $\boldsymbol{v}_1$ and of the tangential component of $\nabla p^{(1)}$. This can be seen as follows. The field dependent pressure gradient $\nabla p^{(1)}$ is a function of y only, then according to relations like

$$\frac{\partial}{\partial x}\frac{\partial p^{(1)}}{\partial y} = 0 = \frac{\partial}{\partial y}\frac{\partial p^{(1)}}{\partial x}$$

the x- and z-components of $\nabla p^{(1)}$ are constant:

$$\nabla p^{(1)} = \boldsymbol{P} + \frac{\partial p^{(1)}}{\partial y}\boldsymbol{u}, \quad \boldsymbol{u}\cdot\boldsymbol{P} = 0, \quad \boldsymbol{P} = \text{const}(\boldsymbol{H}). \tag{1.17}$$

From the tangential component of the modified Navier-Stokes equation [6, 12]

$$\frac{1}{\eta_{iso}}\nabla p - \nabla\cdot\nabla\boldsymbol{v} = -\frac{1}{\eta_{iso}}\frac{p_0}{T_0}\left(c_r + \frac{4}{5}\frac{\omega_0}{\omega_\eta}\right)\nabla T' + \sqrt{2}\,\omega_{\eta T}\nabla\cdot\mathbf{a} + \frac{2}{5}\frac{c_0}{\sqrt{2}}\sqrt{\frac{\omega_b}{\omega_t(1-A_{tr})}}\,a_{bt}(\nabla\nabla\cdot\boldsymbol{B} - \nabla\cdot\nabla\boldsymbol{B})$$

a differential equation for $\boldsymbol{v}_1$ can be derived by subtraction of

$$\frac{1}{\eta_{iso}}\nabla p^{(0)} - \nabla\cdot\nabla\boldsymbol{v}_{iso} = \boldsymbol{0},$$

viz.

$$\frac{1}{\eta_{iso}}\boldsymbol{P} - \nabla\cdot\nabla\boldsymbol{v}_1 = \sqrt{2}\,\omega_{\eta T}(\nabla\cdot\mathbf{a} - \boldsymbol{u}\nabla\cdot(\mathbf{a}\cdot\boldsymbol{u})) - \frac{2}{5}\frac{c_0}{\sqrt{2}}\sqrt{\frac{\omega_b}{\omega_t(1-A_{tr})}}\,a_{bt}\nabla\cdot\nabla(\boldsymbol{B} - \boldsymbol{u}\boldsymbol{u}\cdot\boldsymbol{B}).$$

The quantity of interest is the constant tangentialpressure gradient $\boldsymbol{P}$. Then, in general, also $\boldsymbol{v}_1$ has to be calculated, but a knowledge of $\partial p^{(1)}/\partial y$, T_1 and T_1' is not necessary.

The right hand side of the differential equation for $\boldsymbol{v}_1$ contains derivatives of the tensor polarization $\mathbf{a}$ and the Kagan vector $\boldsymbol{B}$ ($B_\mu = b_{\nu,\nu\mu}$) which are already known from the preceding section. The solution is now written in the following form:

$$\boldsymbol{v}_1(y,\boldsymbol{H}) = -\frac{d^2}{2\,\eta_{iso}}\left(\frac{dp}{dz}\right)_0 A_{\eta T}\boldsymbol{V}(y,\boldsymbol{H}), \quad \boldsymbol{P} = \left(\frac{dp}{dz}\right)_0 A_{\eta T}\boldsymbol{G} \tag{1.18}$$

and

$$\boldsymbol{V}(y,\boldsymbol{H}) = -\left(\frac{y}{d}\right)^2\boldsymbol{G} + \boldsymbol{W} + \sum_{m=-2}^{+2}(2\,\boldsymbol{u}\cdot\mathsf{P}^{(m)}:\overline{\boldsymbol{e}\boldsymbol{u}})^{\tan}\left[\frac{(y/d)^2}{1+i\,m\,\varphi_T} - 2\frac{L_m}{d}\alpha_m(1+(1+i\,m\,\varphi_T)\,a_{Tt})\frac{\cosh(y/L_m)}{\sinh(d/L_m)}\right]. \tag{1.19}$$

Then the mean velocity

$$\bar{\boldsymbol{V}}(\boldsymbol{H}) = \int_{-d}^{+d} \frac{1}{2\,d}\, \boldsymbol{V}(y, \boldsymbol{H})\, \mathrm{d}y$$

is given by

$$\bar{\boldsymbol{V}}(\boldsymbol{H}) = -\frac{1}{3}\,\boldsymbol{G} + \boldsymbol{W} + \sum_{m=-2}^{+2} (2\,\boldsymbol{u}\cdot \mathrm{p}^{(m)} : \overline{\boldsymbol{e}\,\boldsymbol{u}})^{\tan} \left[\frac{\frac{1}{3}}{1+i\,m\,\varphi_{\mathrm{T}}} - 2\left(\frac{L_{\mathrm{m}}}{d}\right)^2 a_m\,(1 + (1+i\,m\,\varphi_{\mathrm{T}})\,a_{\mathrm{Tt}})\right]. \quad (1.20)$$

The quantity $A_{\eta\mathrm{T}} \equiv \omega_{\eta\mathrm{T}}^2/\omega_\eta\,\omega_{\mathrm{T}}$ gives [9, 11] the order of magnitude of the SBE of viscosity [1]. Furthermore, it is the relative difference between the isotropic ($\eta_{\mathrm{iso}} = p_0/\omega_\eta$) and the field free value $\eta = \eta_{\mathrm{iso}}(1 + A_{\eta\mathrm{T}})$ of shear viscosity.

The constant tangential vectors $\boldsymbol{G}$ and $\boldsymbol{W}$ are yet unknown, thus four conditions are needed. Two of them are given by the boundary condition for the tangential velocity $\boldsymbol{v}_1$ [12]:

$$(\boldsymbol{v} + \tfrac{2}{5} p_0^{-1}\, \boldsymbol{q}_{\mathrm{trans}})_1^{\tan} = \frac{l}{\eta_{\mathrm{iso}}}\, C_{\mathrm{m}}\, \boldsymbol{k}_1^{\tan} + \frac{c_0}{\sqrt{3}}\, C_{\mathrm{ma}}\,(\boldsymbol{n}\cdot \underline{\mathbf{b}}\cdot \boldsymbol{n})^{\tan}.$$

Due to the antisymmetry relation $C_{\mathrm{ma}} = -C_{\mathrm{am}}$ the coefficient of thermomagnetic slip C_{ma} is related to C_{am} which describes a production mechanism for the tensor polarization. The tangential force per unit area $\boldsymbol{k}_1^{\tan} = (\bar{\mathbf{p}}_1 \cdot \boldsymbol{n})^{\tan}$ can most simply be calculated by integration of the tangential component of

$$\nabla\cdot \bar{\mathbf{p}}_1 + \nabla\, p^{(1)} = \boldsymbol{O}$$

which is the original form of the Navier-Stokes equation for $\boldsymbol{v}_1$: $\boldsymbol{k}_1^{\tan} = -d\,\boldsymbol{P}$. For the translational heat flux

$$(\boldsymbol{q}_{\mathrm{trans}})_1^{\tan} = \frac{2}{5}\,\frac{T_0}{p_0}\,\lambda_{\mathrm{iso}}^t\,\boldsymbol{P} - \frac{p_0\,c_0}{\sqrt{2}}\,\sqrt{\frac{\omega_{\mathrm{b}}}{\omega_{\mathrm{t}}(1 - A_{\mathrm{tr}})}}\; a_{\mathrm{bt}}\,\boldsymbol{B}^{\tan}$$

has to be inserted [12]. Now, the vector $\boldsymbol{W}$ is related to $\boldsymbol{G}$ through

$$\boldsymbol{W} = \boldsymbol{G}\left(1 + 2\,\frac{l}{d}\,C_{\mathrm{m}} + \frac{4}{5}\,\frac{l_\eta\, l_{\mathrm{t}}}{d^2}\right) + \left(a_{\mathrm{Tt}}\,\frac{L_0}{d}\right)^2 \frac{20}{3}\,(\boldsymbol{e} - \boldsymbol{\Lambda}(\varphi_{\mathrm{b}})\cdot \boldsymbol{e})^{\tan} + \sum_{m=-2}^{+2} (2\,\boldsymbol{u}\cdot \mathrm{p}^{(m)} : \overline{\boldsymbol{e}\,\boldsymbol{u}})^{\tan} \quad (1.21)$$

$$\cdot \left\{\frac{-1}{1+i\,m\,\varphi_{\mathrm{T}}} + 2\,a_{\mathrm{m}}\,\frac{L_{\mathrm{m}}}{d}\,[1 - (1+i\,m\,\varphi_{\mathrm{T}})\,\tilde{C}_{\mathrm{ma}}]\,\coth\frac{d}{L_{\mathrm{m}}} + 2\left(\frac{L_{\mathrm{m}}}{d}\right)^2 [\tilde{C}_{\mathrm{ma}}\,(1 + (1+i\,m\,\varphi_{\mathrm{T}})\,a_{\mathrm{Tt}}) + a_{\mathrm{Tt}}]\right\}.$$

Notice, that $\boldsymbol{\Lambda}$ (φ_b) essentially determines the heat conductivity tensor [12].

In order to get a further relation between $\boldsymbol{G}$ and $\boldsymbol{W}$ we remember that the real capillary used in experiments [3, 4] is closed in x-direction. Hence, for the model of infinite parallel plates we impose the condition $(\boldsymbol{u}\times\boldsymbol{e})\cdot\bar{\boldsymbol{v}}_1 = 0$.

From Eq. (1.20) we get (1.22)

$$\boldsymbol{W}\cdot(\boldsymbol{u}\times\boldsymbol{e}) = \tfrac{1}{3}\,\boldsymbol{G}\cdot(\boldsymbol{u}\times\boldsymbol{e}) - \sum_{m=-2}^{+2} 2\,(\boldsymbol{u}\times\boldsymbol{e}\,\boldsymbol{u}) : \mathrm{p}^{(m)} : \overline{\boldsymbol{e}\,\boldsymbol{u}}\left[\frac{\frac{1}{3}}{1+i\,m\,\varphi_{\mathrm{T}}} - 2\left(\frac{L_{\mathrm{m}}}{d}\right)^2 a_m\,(1 + (1+i\,m\,\varphi_{\mathrm{T}})\,a_{\mathrm{Tt}})\right].$$

Finally, a relation between the z-components of $\boldsymbol{W}$ and $\boldsymbol{G}$ is derived from the fact that the measuring capillary is part of a gas-flow Wheatstone bridge [2, 4]. Then

$$\overline{\boldsymbol{v}^H(y)} = \overline{\boldsymbol{v}_1(y,\boldsymbol{H})} - \overline{\boldsymbol{v}_1(y,\boldsymbol{0})} = -\,\delta{*}\,\boldsymbol{G}\cdot\boldsymbol{e}\,A_{\eta\mathrm{T}}\,\overline{\boldsymbol{v}_{\mathrm{iso}}(y)}$$

applies (see Appendix B). For $\delta = 0$ the gas flow is kept constant if the magnetic field is switched on. Similarly, for $\delta = 1$ the pressure difference over the ideal bridge is kept constant, or for $\delta \to \infty$ the pressure difference over the measuring capillary (i.e. $\boldsymbol{G}\cdot\boldsymbol{e} = 0$). The result is stated as follows:

$$\boldsymbol{e}\;\boldsymbol{W}(\boldsymbol{H}) - \boldsymbol{e}\cdot\boldsymbol{W}(\boldsymbol{0}) = -\frac{1}{3}\,\boldsymbol{e}\cdot\boldsymbol{G}\left[2\,\delta - 1 + 6\,\delta\,\frac{l}{d}\,C_{\mathrm{m}} + \frac{12}{5}\,\delta\,\frac{l_\eta\,l_{\mathrm{t}}}{d^2}\right] + \sum_{m=-2}^{+2} 2\,(\boldsymbol{e}\,\boldsymbol{u}) : \mathrm{p}^{(m)} : \overline{\boldsymbol{e}\,\boldsymbol{u}}$$

$$\cdot\left[\frac{\frac{1}{3}\,i\,m\,\varphi_{\mathrm{T}}}{1+i\,m\,\varphi_{\mathrm{T}}} + 2\,a_m\left(\frac{L_{\mathrm{m}}}{d}\right)^2 (1 + (1+i\,m\,\varphi_{\mathrm{T}})\,a_{\mathrm{Tt}}) - 2\,a_0\left(\frac{L_0}{d}\right)^2 (1 + a_{\mathrm{Tt}})\right]. \quad (1.23)$$

By comparison of Eqs. (1.23) and (1.22) with Eq. (1.21) the constant vector $\mathbf{G}$ is obtained in the form (see Appendix A):

$$(1+\delta)\,\mathbf{G}\cdot\boldsymbol{e} = (1+\delta)\,G_z = F_1'(h_y^2+h_z^2-4\,h_y^2\,h_z^2) + F_2'(1-h_y^2)\,(1-h_z^2) + \frac{3\,(a_{\mathrm{Tt}}(L_0/d))^2}{1+3\,(l/d)\,C_{\mathrm{m}}+\frac{6}{5}l_\eta\,l_{\mathrm{t}}/d^2}\left[\frac{\varphi_b^2}{1+\varphi_b^2}\,(1+2\,h_z^2)+\frac{8\,\varphi_b^2}{1+4\,\varphi_b^2}\,(1-h_z^2)\right], \tag{1.24}$$

$$\mathbf{G}\cdot(\boldsymbol{u}\times\boldsymbol{e}) \equiv \mathbf{G}_x = h_x\,h_z[F_1'(1-4\,h_y^2)+F_2'(h_y^2-1)] + h_y[F_1''(2\,h_y^2-1)+F_2''(1-h_y^2)] + \frac{3\,(a_{\mathrm{Tt}}(L_0/d))^2}{1+3\,(l/d)\,C_{\mathrm{m}}+\frac{6}{5}l_\eta\,l_{\mathrm{t}}/d^2}\left[h_x\,h_z\left(\frac{\varphi_b^2}{1+\varphi_b^2}-\frac{8\,\varphi_b^2}{1+4\,\varphi_b^2}\right)+h_y\left(\frac{\varphi_b}{1+\varphi_b^2}\,\frac{4\,\varphi_b}{1+4\,\varphi_b^2}\right)\right]. \tag{1.25}$$

Here, $h_x = \boldsymbol{h}\cdot(\boldsymbol{u}\times\boldsymbol{e})$, $h_y = \boldsymbol{h}\cdot\boldsymbol{u}$, $h_z = \boldsymbol{h}\cdot\boldsymbol{e}$ are the components of the unit vector $\boldsymbol{h}$ in the direction of the magnetic field. The quantities F_m', F_m'' are the real and imaginary parts of the complex functions

$$F_m = F_m' + i\,F_m'' = (\tilde{F}_m-\tilde{F}_0)/(1+3\,(l/d)\,C_{\mathrm{m}}+\tfrac{6}{5}l_\eta\,l_{\mathrm{t}}/d^2) \tag{1.26}$$

with ($m = 0, \pm 1, \pm 2$)

$$\tilde{F}_m = \frac{1}{1+i\,m\,\varphi_{\mathrm{T}}} - 3\,a_{\mathrm{m}}\,\frac{L_{\mathrm{m}}}{d}\coth\frac{d}{L_{\mathrm{m}}}\,(1-(1+i\,m\,\varphi_{\mathrm{T}})\,\tilde{C}_{\mathrm{ma}}) + 3\,a_{\mathrm{m}}\left(\frac{L_{\mathrm{m}}}{d}\right)^2(1+(1+i\,m\,\varphi_{\mathrm{T}})\,a_{\mathrm{Tt}}) - 3\left(\frac{L_{\mathrm{m}}}{d}\right)^2[\tilde{C}_{\mathrm{ma}}(1+(1+i\,m\,\varphi_{\mathrm{T}})\,a_{\mathrm{Tt}})+a_{\mathrm{Tt}}]\,. \tag{1.27}$$

According to Eq. (1.24) the pressure gradient G_z depends on the value of δ. But the quantity measured in a gas-flow Wheatstone bridge is proportional to $(1+\delta)\,G_z$, hence it is independent of δ (see Appendix B).

II. Discussion of Pressure Gradient and Flow Velocity

In this section the pressure gradient $\boldsymbol{P}$ and the flow velocity $\boldsymbol{v}_1$ are evaluated up to terms linear in the mean free path. Then Eqs. (1.24), (1.25) reduce to

$$(1+\delta)\,G_z = F_1'(h_y^2+h_z^2-4\,h_y^2\,h_z^2) + F_2'(1-h_y^2)\,(1-h_z^2)\,, \tag{2.1}$$

$$G_x = h_x\,h_z\,[F_1'(1-4\,h_y^2)+F_2'(h_y^2-1)] + h_y[F_1''\,(2\,h_y^2-1)+F_2''\,(1-h_y^2)]\,, \tag{2.2}$$

and in F_m', F_{m}'' all terms which are of higher than first order in l/d, L_0/d are neglected. In this approximation the angular dependence of the pressure gradient $\mathbf{G}$, as described by Eqs. (2.1), (2.2), is independent of the mean free path.

This is not the case for higher approximations of Eqs. (1.24), (1.25). Then terms proportional to $(a_{\mathrm{Tt}}\,L_0/d)^2$ occur, which have an angular dependence different from that in Eqs. (2.1), (2.2). But for the experimental conditions [3, 4] (see Section III) these are minor corrections and shall not be discussed here.

If one is interested in the pressure gradient $\mathbf{G}$ only, the heat fluxes may be neglected throughout since they contribute higher order terms like $l_\eta\,l_{\mathrm{t}}/d^2$ and $a_{\mathrm{Tt}}(L_0/d)^2$. In contradistinction, the heat fluxes give (via the vector $\boldsymbol{a}^{\mathrm{rt}}$) contributions of the order L_0/d to the tensor polarization $\mathbf{a}$ and to the anisotropic velocity $\boldsymbol{v}_1$.

(a) The Hydrodynamic Limit

For vanishing mean free path Eqs. (1.26), (1.27) yield the simple result

$$(F_m)_{p_0\to\infty} \equiv F_m^{\infty} = -\frac{(m\,\varphi_{\mathrm{T}})^2}{1+(m\,\varphi_{\mathrm{T}})^2} - i\,\frac{m\,\varphi_{\mathrm{T}}}{1+(m\,\varphi_{\mathrm{T}})^2}\,. \tag{2.3}$$

The five viscosity coefficients can be expressed by the functions F_m^∞ $(m=0, \pm 1, \pm 2)$, then Eqs. (2.1) – (2.3) summarize the wellknown results derived (for $\delta=0$) by various authors [11, 17]. These formulas have been used, together with Eq. (1.18), for the evaluation of SBE measurements [1, 3, 4], i. e. for a determination of $A_{\eta\mathrm{T}}$ and ω_T.

The vector $\boldsymbol{G}$ can be expressed by (see Appendix A)

$$\boldsymbol{G}^{(0)} \equiv \sum_{m=-2}^{+2} \frac{1}{1+i\,m\,\varphi_\mathrm{T}} \left(2\,\boldsymbol{u}\cdot\mathcal{P}^{(m)} : \overline{\boldsymbol{e}\,\boldsymbol{u}}\right)^{\tan} - \boldsymbol{e} \quad (2.4)$$

through the relation

$$G_x = G_x^{(0)}, \quad G_z = \frac{1}{1+\delta}\, G_z^{(0)}. \quad (2.5)$$

By the use of Eq. (1.21), viz.

$$\boldsymbol{W} = \boldsymbol{G} - \boldsymbol{G}^{(0)} - \boldsymbol{e} = -\boldsymbol{e}\left(1 + \frac{\delta}{1+\delta}\, G_z^{(0)}\right),$$

the anisotropic velocity is obtained from Eq. (1.19) as

$$\boldsymbol{V}(y,\boldsymbol{H}) = -\boldsymbol{e}\left(1-\left(\frac{y}{d}\right)^2\right)\left(1+\frac{\delta}{1+\delta}\, G_z^{(0)}\right). \quad (2.6)$$

For $l/d=0$ the velocity has only a z-component, hence its x-component is at least of order l/d.

The parabolic velocity profile in Eq. (2.6) is multiplied by a function which depends on the choice of δ and on the magnetic field. For $\delta \neq 0$ (i. e. $\delta=1$ or $\delta\to\infty$) the mass flow through the capillary changes with the magnetic field $\boldsymbol{H}$ (see Appendix B). Thus, the field dependent part

$$\boldsymbol{V}^H(y) = -\boldsymbol{e}\left(1-\left(\frac{y}{d}\right)^2\right)\frac{\delta}{1+\delta}\, G_z^{(0)}$$

of the flow velocity is nonzero. But for $\delta=0$ this field induced velocity vanishes:

$$\boldsymbol{V}^H(y) = \boldsymbol{0}, \quad \boldsymbol{V}(y,\boldsymbol{H}) = \boldsymbol{V}^0(y) = -\boldsymbol{e}\left(1-\left(\frac{y}{d}\right)^2\right).$$

Then $\boldsymbol{V}^H(y)$ is of order l/d, which is plausible since for $\delta=0$ the two conditions $\overline{\boldsymbol{V}^H}=\boldsymbol{0}$ and $\boldsymbol{V}^H(\pm d)=\boldsymbol{0}$ have to be fulfilled.

In general, the total velocity $\boldsymbol{v}$ is proportional to the total pressure gradient in z-direction

$$\boldsymbol{e}\cdot\nabla p = \boldsymbol{e}\cdot\nabla p^{(0)}\,(1+A_{\eta\mathrm{T}}\,G_z), \text{ i. e.}$$

$$\boldsymbol{v}(y,\boldsymbol{H}) = -\frac{d^2}{2\,\eta_\mathrm{eff}}\left(1-\left(\frac{y}{d}\right)^2\right)\boldsymbol{e}\cdot\nabla p\,\boldsymbol{e}. \quad (2.7)$$

Here, the effective field dependent viscosity coefficient

$$\eta_\mathrm{eff} = \eta\,(1+A_{\eta\mathrm{T}}\,G_z^{(0)}) \quad (2.8)$$

and the field free value of shear viscosity $\eta = \eta_\mathrm{iso}\,(1+A_{\eta\mathrm{T}})$ are correct in first order in the small quantity $A_{\eta\mathrm{T}}$. In a gas-flow Wheatstone bridge the relative change of viscosity through a magnetic field

$$\frac{\Delta\eta}{\eta} \equiv \frac{\eta_\mathrm{eff}-\eta}{\eta} = A_{\eta\mathrm{T}}\,G_z^{(0)}$$

is measured [1–4] (see Appendix B). Notice, that this quantity is independent of δ, despite the fact that the pressure gradient G_z and the field induced velocity $\boldsymbol{V}^H(y)$ strongly depend on δ.

(b) Linear Knudsen Corrections

In this section the pressure gradient and the anisotropic velocity are evaluated up to terms which are linear in the mean free path. First, the expression (1.11) for a_m is simplified by replacing $\coth d/L_\mathrm{m}$ by 1, then the right hand side of Eqs. (1.26), (1.27) is linearized with respect to l/d and L_0/d [7]:

$$F_m = F_m^\infty\left(1-3\,\frac{l}{d}\,C_\mathrm{m}\right) - 3\,\frac{L_0}{d}\left[\frac{\left(\dfrac{1}{1+i\,m\,\varphi_\mathrm{T}}-\tilde{C}_\mathrm{ma}\right)^2}{\tilde{C}_\mathrm{a}+\sqrt{\dfrac{1+i\,m\,\varphi_\mathrm{b}}{1+i\,m\,\varphi_\mathrm{T}}}} - \frac{(1-\tilde{C}_\mathrm{ma})^2}{\tilde{C}_\mathrm{a}+1}\right]. \quad (2.9)$$

Use has been made of the antisymmetry relation [12] $\tilde{C}_\mathrm{am} = -\tilde{C}_\mathrm{ma}$.

1) Flow Velocity

Now the anisotropic velocity is calculated in linear approximation in the mean free path from Eqs. (1.19), (1.21). Its field free part

$$\boldsymbol{V}^0(y) = V_z^0(y)\,\boldsymbol{e},\ V_z^0(y) = -\left(1-\left(\frac{y}{d}\right)^2\right) + 2\,\frac{L_0}{d}\,\frac{1-\tilde{C}_\mathrm{ma}}{1+\tilde{C}_\mathrm{a}}\left[1-\tilde{C}_\mathrm{ma}-(1+a_\mathrm{Tt})\,\frac{\cosh(y/L_0)}{\cosh(d/L_0)}\right]$$

gives only a negligibly small contribution to

$$\boldsymbol{v}(y,\boldsymbol{O}) = -\frac{d^2}{2\,\eta_{\text{iso}}}\left(\frac{\mathrm{d}p}{\mathrm{d}z}\right)_0 \boldsymbol{e}\left[1-\left(\frac{y}{d}\right)^2 + 2\,\frac{l}{d}\,C_{\text{m}} + A_{\eta\text{T}}\,V_z^0(y)\right]$$

and

$$\overline{\boldsymbol{v}(y,\boldsymbol{O})} = -\frac{d^2}{3\,\eta_{\text{iso}}}\left(\frac{\mathrm{d}p}{\mathrm{d}z}\right)_0 \boldsymbol{e}\left[1+3\,\frac{l}{d}\,C_{\text{m}} + \frac{3}{2}\,A_{\eta\text{T}}\,\overline{V_z^0(y)}\right]. \tag{2.11}$$

We are interested here mainly in the field dependent velocity:

$$V_x^H(y) = h_x h_z [D_1'(1-4\,h_y^2) + D_2'(h_y^2-1)] + h_y\,[D_1''(2\,h_y^2-1) + D_2''(1-h_y^2)]\,,$$
$$V_z^H(y) = D_1'(h_y^2+h_z^2-4\,h_y^2\,h_z^2) + D_2'(1-h_y^2)\,(1-h_z^2)\,. \tag{2.12}$$

For $\delta \neq 0$ those terms in D_m', D_m'' which are proportional to the mean free path give only small corrections of the high pressure values in Eq. (2.6). But for $\delta = 0$ the velocity $\boldsymbol{V}^H(y)$ vanishes in the high pressure limit since it is of order l/d. From now on, the discussion of $\boldsymbol{V}^H(y)$ is restricted to the case $\delta = 0$. The functions D_m' and D_m'' are then the real and imaginary parts of

$$D_m = D_m' + i\,D_m'' = \left(\frac{1}{3}-\left(\frac{y}{d}\right)^2\right)(F_m - F_m^\infty) \tag{2.13}$$
$$+2\,\frac{L_0}{d}\left\{\frac{\cosh(y/L_0)}{\cosh(d/L_0)}\;\frac{(1-\tilde{C}_{\text{ma}})\,(1-a_{\text{Tt}})}{1+\tilde{C}_{\text{a}}} - \frac{\cosh(y/L_{\text{m}})}{\cosh(d/L_{\text{m}})}\;\frac{\left(\dfrac{1}{1+i\,m\,\varphi_{\text{T}}}-\tilde{C}_{\text{ma}}\right)\left(\dfrac{1}{1+i\,m\,\varphi_{\text{T}}}+a_{\text{Tt}}\right)}{\sqrt{(1+i\,m\,\varphi_{\text{b}})/(1+i\,m\,\varphi_{\text{T}})}+\tilde{C}_{\text{a}}}\right\}.$$

The value of $\boldsymbol{V}^H(y)$ at the walls $(y = \pm d)$ is given by mechanical $(\propto C_{\text{m}})$, by thermomagnetic $(\propto \tilde{C}_{\text{ma}})$, and by thermal $(\propto a_{\text{Tt}})$ slip. The spatial dependence of $\boldsymbol{V}^H(y)$ is determined by two essentially different terms, viz. one term which is proportional to $\frac{1}{3} - (y/d)^2$ and a second term which contains the hyperbolic functions $\cosh(y/L_0)/\cosh(d/L_0)$ and $\cosh(y/L_{\text{m}})/\cosh(d/L_{\text{m}})$. Near the walls both terms are of same importance, within the gas (e. g. at $y = 0$) only $\frac{1}{3} - (y/d)^2$ survives, the hyperbolic terms are negligibly small. These exponentially decaying contributions are due to the peculiar behaviour of the tensor polarization in a small boundary layer near the walls (see Figure 2). For $\boldsymbol{h} = \boldsymbol{u}$ we have according to Eq. (2.12)

$$V_x^H(y) = D_1'', \quad V_z^H(y) = D_1'.$$

These functions are calculated for HD from Eq. (2.13) with the parameters taken from Table 2 and Table 3, with $L_0/d = 0.1$ and for three values of φ_{T} (i. e. of H/p_0). The result is plotted in Figure 3. Halfway between the plates (and for $\varphi_{\text{T}} = 0.3,\ 2.0$) the velocity components are positive, i. e. $V_x^H(0) > 0$, $V_z^H(0) > 0$. Then $\boldsymbol{v}^H(0)$ has components parallel to $\boldsymbol{v}(0,\boldsymbol{0})$ and $\boldsymbol{h}\times\boldsymbol{v}(0,\boldsymbol{0})$.

2) Pressure Gradient

Those terms in F_m, Eq. (2.9), which are proportional to the mean free path give rise to Knudsen corrections for the pressure gradient $\boldsymbol{P}$.

In the hydrodynamic limit $(l/d = 0)$ half of the saturation value $F_{\text{m}}'^{\infty}(\varphi_{\text{T}}\to\infty) \equiv F_{\text{sat}}^{\infty} = -1$ is reached at $(m\,\varphi_{\text{T}})_{1/2}^{\infty} = 1$. For $l/d > 0$ the absolute saturation value is smaller than 1,

$$F_{\text{sat}} = \frac{-1}{1+N_{\text{S}}\,l/d}\,, \quad N_{\text{S}} = 3\,C_{\text{m}} + 3\,\frac{L_0}{l}\left[\frac{(1-\tilde{C}_{\text{ma}})^2}{1+\tilde{C}_{\text{a}}} - \frac{\tilde{C}_{\text{ma}}^2}{\sqrt{\varkappa}+\tilde{C}_{\text{a}}}\right], \tag{2.14}$$

and $\frac{1}{2}\,F_{\text{sat}}$ is reached at

$$(m\,\varphi_{\text{T}})_{1/2} = 1 + n_{\text{S}}\,l/d\,, \quad n_{\text{S}} = 3\,\frac{L_0}{l}\left[\frac{(1-\tilde{C}_{\text{ma}})^2}{1+\tilde{C}_{\text{a}}} + \frac{\tilde{C}_{\text{ma}}^2}{\sqrt{\varkappa}+\tilde{C}_{\text{a}}} + \text{Real}\left(\frac{i(1-2\,\tilde{C}_{\text{ma}})+2\,\tilde{C}_{\text{ma}}}{\sqrt{\dfrac{1+i\varkappa}{1+i}}+\tilde{C}_{\text{a}}}\right)\right] \tag{2.15}$$

which is greater than 1. Here $\varkappa$ denotes the ratio $\varkappa = \omega_{\text{T}}/\omega_b$.

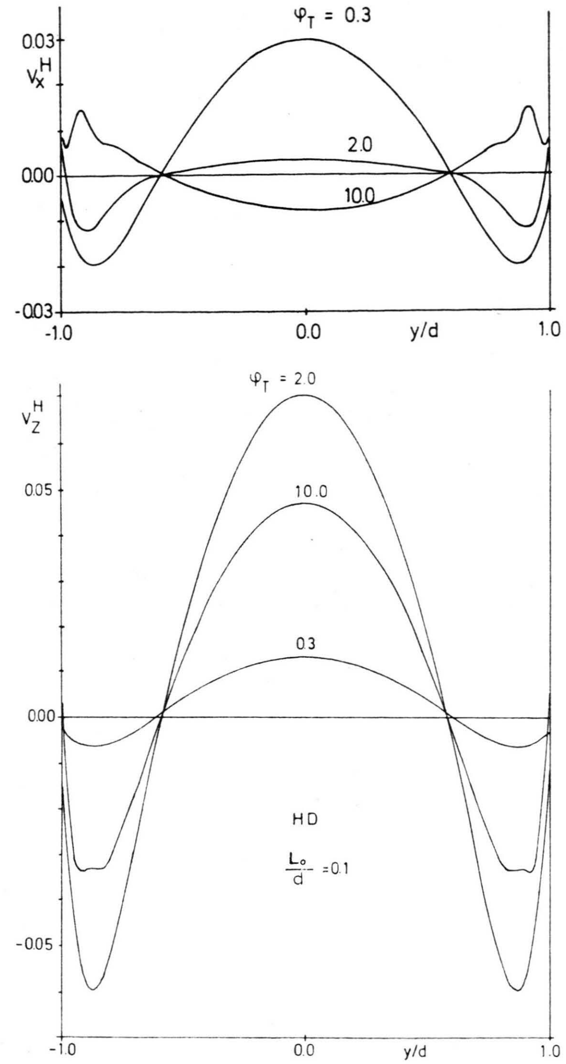

Fig. 3. Spatial dependence of the magnetic field dependent velocity $\boldsymbol{V}^H(y)$ in HD for $\delta=0$, $L_0/d=0.1$, $\boldsymbol{h}=\boldsymbol{u}$, and $\varphi_T=0.3$, 2.0, 10.0; $V_x{}^H(y)=D_1''$, $V_z{}^H(y)=D_1'$. The functions D_1', D_1'' are calculated from Eq. (2.13) by use of Table 2, Table 3.

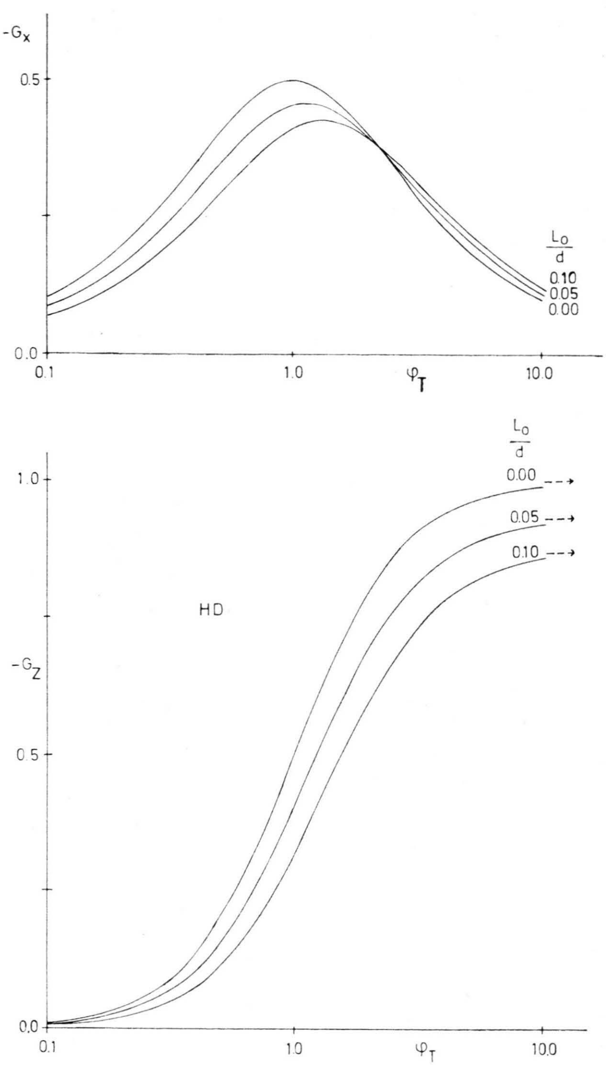

Fig. 4. Knudsen corrections for the pressure gradients in HD for $\boldsymbol{h}=\boldsymbol{u}$ and $L_0/d=0.05$, 0.10; $G_x=F_1''$, $G_z=F_1'$. The functions F_1', F_1'' are calculated from Eq. (2.9) with the parameters from Table 2, Table 3. The saturation values F_{sat} are indicated by arrows, see Equation (2.14).

Similarly, the height and position of the maximum of $-F_m''$ are shifted from the hydrodynamic values $F^{\infty}_{\text{Max}}=-\frac{1}{2}$, $(m\,\varphi_T)^{\infty}_{\text{Max}}=1$ to

$$F_{\text{Max}}=\frac{-1/2}{1+N_{\text{M}}\,l/d}\,,\quad N_{\text{M}}=3\,C_{\text{m}}+3\,\frac{L_0}{l}\,\text{Im}\left(\frac{i(1-2\,\tilde C_{\text{ma}})+2\,\tilde C_{\text{ma}}(1-\tilde C_{\text{ma}})}{\sqrt{\dfrac{1+i\varkappa}{1+i}}+\tilde C_{\text{a}}}\right), \tag{2.16}$$

and $(m\,\varphi_T)_{\text{Max}}=1+n_{\text{M}}\,l/d\,,$

$$n_{\text{M}}=3\,\frac{L_0}{l}\,\text{Im}\left[\frac{i+2\,\tilde C_{\text{ma}}-1}{\sqrt{\dfrac{1+i\varkappa}{1+i}}+\tilde C_{\text{a}}}-\frac{1-\varkappa}{4}\sqrt{\frac{1+i}{1+i\varkappa}}\;\frac{i(1-2\,\tilde C_{\text{ma}})+2\,\tilde C_{\text{ma}}(1-\tilde C_{\text{ma}})}{\left(\sqrt{\dfrac{1+i\varkappa}{1+i}}+\tilde C_{\text{a}}\right)^2}\right]. \tag{2.17}$$

Notice, that the shifting parameters n_S and n_M do not depend on C_m, they are determined by C_a and $\tilde{C}_{am} = -\tilde{C}_{ma}$ only which characterize the behaviour of the tensor polarization near the wall.
In general, the shape of the curves $F_m'(\varphi_T)$, $F_m''(\varphi_T)$ will be slightly different from that of the hydrodynamic limits $\frac{-(m\varphi_T)^2}{1+(m\varphi_T)^2}$ and $\frac{-m\varphi_T}{1+(m\varphi_T)^2}$. But this is not the case for $\varkappa = 1$. Then the Knudsen corrections for $\boldsymbol{P}$ can be obtained from the hydrodynamical limit by replacing all relaxation constants by their effective values [7] which are the sum of a gas-gas and a gas-wall collision frequency. Furthermore, the correction factors are then equal for F_m' and F_m'',

$$\varkappa = 1: n_S = n_M = 3\frac{L_0}{l}\frac{1}{1+\tilde{C}_a}, \quad N_S = N_M = 3\,C_m + 3\frac{L_0}{l}\frac{1-2\,\tilde{C}_{ma}}{1+\tilde{C}_a}. \tag{2.18}$$

In this case the shifting factors n_S and n_M are determined by the positive coefficient $\tilde{C}_a$ alone which describes the accommodation of tensor polarization. Besides $\tilde{C}_a$, the reduction factors N_S and N_M contain also the coefficients $\tilde{C}_{ma}$ and C_m of thermomagnetic and of mechanical slip.

Experimental data on Knudsen corrections for the SBE of viscosity [3, 4] show that all four parameters n_S, N_S, n_M, N_M are positive, e. g. with increasing Knudsen number l/d the maximum of $-F_m''$ becomes smaller and is reached at higher $m\,\varphi_T$-values.

According to Eqs. (2.1), (2.2) the pressure gradients are given by $G_x = F_1''$, $G_z = F_1'$, if $\boldsymbol{h} = \boldsymbol{u}$ and $\delta = 0$ apply. In Fig. 4 G_x and G_z are plotted versus φ_T for three values of L_0/d. The functions F_1' and F_1'' are calculated for HD from Eq. (2.9) with the parameters from Table 2 and Table 3.

III. Comparison with Experimental Data

Measurements of the SBE of viscosity have been done by Hulsman et al. [3, 4] with a flat rectangular capillary of length D_z, width D_x and thickness D_y. The condition $D_z \gg D_x \gg D_y$ applies, e. g. a box with [3]

$$D_z = 100\text{ mm}, \quad D_x = 10\text{ mm}, \quad D_y = 0.5\text{ mm}$$

has been used. Hence, theoretical results obtained for infinite parallel plates of distance $D_y = 2\,d$ may be compared with the experimental data of Hulsman et al. [3, 4].

In Table 1 the five parameters n_α, n_β^{tr}, n_γ^{tr}, n_β^{long}, n_γ^{long} which characterize the observed Knudsen corrections [3, 4] are given for the gases HD, CH_4, CO and N_2. The increase of the field free gas flow due to slip effects is described by the factor $1 + n_\alpha\,l/D_y$, i. e. n_α should be proportional to the mechanical slip coefficient C_m [neglecting the term $A_{\eta T}\,\overline{V_z^0(y)}$ in Eq. (2.11)],

$$\tfrac{1}{6} n_\alpha \triangleq C_m\,. \tag{3.1}$$

Similar corrections have been applied to the field dependent pressure gradient $\boldsymbol{P}$. In detail, by use of Eqs. (2.1), (2.2) and (1.18) the quantities $(F_m')_{exp}$ and $(F_m'')_{exp}$ have been extracted from the measured gradients $\boldsymbol{P}$. Then, the formulas [4]

$$(F_m')_{exp} = -\frac{(m\,\psi_l)^2}{1+(m\,\psi_l)^2}\,\frac{1}{1+n_\beta^{long}\,l/D_y}\,, \qquad \psi_l = \frac{\varphi_T}{1+n_\gamma^{long}\,l/D_y}\,, \tag{3.2}$$

and [3]

$$(F_m'')_{exp} = -\frac{m\psi_t}{1+(m\,\psi_t)^2}\,\frac{1}{1+n_\beta^{tr}\,l/D_y}\,, \qquad \psi_t = \frac{\varphi_T}{1+n_\gamma^{tr}\,l/D_y} \tag{3.3}$$

have been used in order to account for the Knudsen corrections. Consequently the effect is reduced by the same factor for all φ_T-values, and the H/p_0-axis is simply stretched. As we have seen in the preceding section this procedure is, strictly speaking, only correct for $\varkappa = 1$, since for $\varkappa \neq 1$ the shape of the curves may also change.

A first estimate for the coefficients C_m, $\tilde{C}_a$, $\tilde{C}_{ma}$ can be obtained by comparison of Eqs. (3.2), (3.3) for $\psi_l = 1 = \psi_t$ with Eqs. (2.14) – (2.17). Then the correspondence

$$\tfrac{1}{2}\,n_\beta^{long} \triangleq N_S\,, \quad \tfrac{1}{2}\,n_\gamma^{long} \triangleq n_S\,, \quad \tfrac{1}{2}\,n_\beta^{tr} \triangleq N_M\,, \quad \tfrac{1}{2}\,n_\gamma^{tr} \triangleq n_M \tag{3.4}$$

should hold. In Fig. 5 the variation of N_S, n_S, N_M and n_M with $\tilde{C}_{ma}$ and $\tilde{C}_a$ is shown for HD and $C_m = 1.0$. Remember, that n_M and n_S do not depend on C_m. The parameters $\varkappa = \omega_T/\omega_b$ and L_0/l occurring in Eqs. (2.14) – (2.17) have been inferred [12] from SBE data [2–5]. They are given for HD, CH_4, CO and N_2 in Table 2 together with $|\omega_{\eta T}|/\omega_T$, $A_{\eta T}$ and a_{Tt}. By comparison of N_S, n_S, N_M, n_M with the experimental quantities $\frac{1}{2} n_\beta^{long}$, $\frac{1}{2} n_\gamma^{long}$, $\frac{1}{2} n_\beta^{tr}$, $\frac{1}{2} n_\gamma^{tr}$ a certain range of variation of the parameters C_m, $\tilde{C}_a$, $\tilde{C}_{ma}$ can be obtained.

The four correction factors N_S, n_S, n_M and n_M are expressed by the three surface parameters C_m, $\tilde{C}_a$ and $\tilde{C}_{ma}$ (notice $\tilde{C}_{am} = -\tilde{C}_{ma}$), hence they are not independent of each other. In particular, the ratios N_S/N_M and n_S/n_M are not very different from 1 for CH_4, CO and N_2; e. g. for N_2 the inequalities $0.93 < N_S/N_M < 0.98$, $1.02 < n_S/n_M < 1.06$ apply, if the parameters $\tilde{C}_a$, $\tilde{C}_{ma}$ vary in the range $0.4 \leqq \tilde{C}_a \leqq 1.0$, $0.0 \leqq \tilde{C}_{ma} \leqq 0.5$. Thus the experimental value of $n_\gamma^{long}/n_\gamma^{tr} = 2$ for N_2 ($\varkappa = 0.47$) cannot be understood within the framework of the present theory. According to (2.18) $n_S/n_M = 1 = N_S/N_M$ applies for $\varkappa = 1$. For all four gases HD, CH_4, CO and N_2 the inequalities $N_S/N_M < 1$, $n_S/n_M > 1$ hold in the parameter range indicated above.

The final determination of C_m, $\tilde{C}_a$, $\tilde{C}_{ma}$ is performed by minimizing the relative deviation between theoretical and experimental curves, i. e. by comparing Eqs. (2.9) with Eqs. (3.2), (3.3) for a number of φ_T-values $\varphi_1, \ldots, \varphi_N$. The relative quadratic deviations

$$Q' = \left[\frac{1}{N} \sum_{k=1}^{N} \left(\frac{F_m' - (F_m')_{exp}}{(F_m')_{exp}}\right)^2_{m\varphi_T = \varphi_\kappa}\right]^{1/2}, \quad Q'' = \ldots$$

depend on the choice of $\varphi_1, \ldots, \varphi_N$, on the Knudsen number l/d and on the parameters C_m, $\tilde{C}_a$, $\tilde{C}_{ma}$. For a fixed set of $\varphi_1, \ldots, \varphi_N$ the Knudsen parameters C_m, $\tilde{C}_a$, $\tilde{C}_{ma}$ are chosen such [6] that Q' and Q'' are as small as possible for all Knudsen numbers in the range $0.005 \leqq l/d \leqq 0.05$ (which corresponds roughly [6] to experimental conditions [3,4]). A suitable set of values for C_m, $\tilde{C}_a$, $\tilde{C}_{ma}$ (and C_a, C_{ma}) is given in Table 3 together with the corresponding values for N_S, n_S, N_M, n_M. A variation of ± 0.05 in $\tilde{C}_a$, $\tilde{C}_{ma}$ is possible. Typical values for Q', Q'' at $l/d = 0.05$ are about [6] 1% to 3%, with the exception of $Q' = 15\%$ for HD (but $Q' = 3\%$ at $l/d = 0.025$).

The coefficient of mechanical slip C_m is related to the accommodation of tangential momentum at the wall. Its value is very close to 1, in accordance with $n_a = 6$. Similarly, the parameter C_a describes the accommodation of tensor polarization at the wall. It is found to be of order 1, and this is confirmed by Halbritter's theoretical results [15]. The coefficient C_{am} characterizes the production of tensor polarization by gas-wall collisions as well as thermomagnetic slip ($C_{ma} = -C_{am}$). It is at least one order of magnitude smaller than C_a. For the gases CH_4, CO, N_2

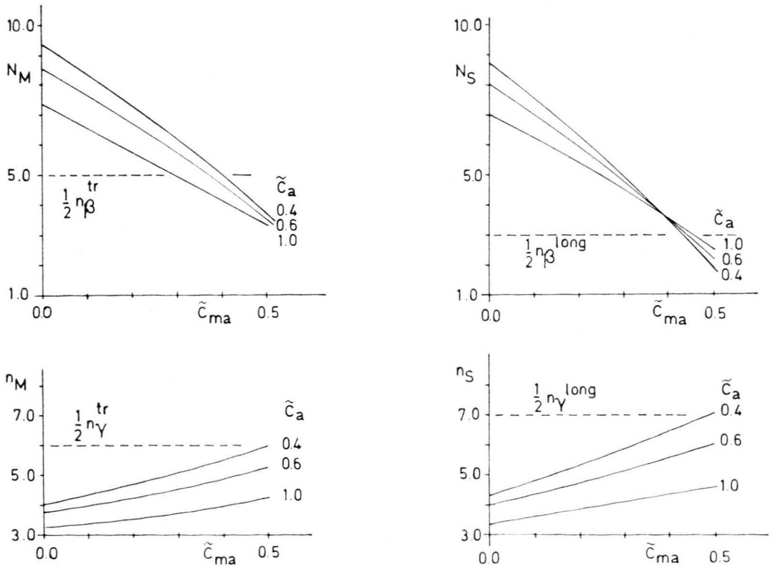

Fig. 5. Dependence of the correction factors N_M, n_M, N_S, n_S on the surface parameters $\tilde{C}_{ma}$ and $\tilde{C}_a$ for HD with $C_m = 1.0$, see Eqs. (2.14) – (2.17). The dotted lines refer to the experimental values of [3] $\frac{1}{2} n_\beta^{tr}$, $\frac{1}{2} n_\gamma^{tr}$ and [4] $\frac{1}{2} n_\beta^{long}$, $\frac{1}{2} n_\gamma^{long}$ cf. Table 1 and Eq. (3.4); $\varkappa = 0.16$ and $L_0/l = 2.68$ have been taken from Table 2.

the parameter $\tilde{C}_{am}$ practically plays no role, e. g. $\tilde{C}_{am}=0$ or $\tilde{C}_{am}=\pm 0.05$, i. e. $C_{am}=0$ or $C_{am}=\pm 0.0045$ (for CO, N_2) are possible values. But for HD we have $\tilde{C}_{ma}=0.4$, i. e. $C_{ma}=0.07$ is about a factor of 15 larger than for CO and N_2. Due to Halbritter [15], C_{am} can be related to the noncentral part of the interaction potential between a gas molecule and a potential wall.

Knudsen corrections for flow birefringence in gases can be calculated [14] from the same set of constitutive laws, differential equations and boundary conditions used in the present paper. Since the same set of parameters C_m, C_a, C_{am} occurs there are relations between both types of Knudsen corrections which could be tested experimentally. Furthermore, C_a and C_{ma} also play a role (besides other surface parameters) for the theory of thermomagnetic pressure difference [6, 7]. The theory is thought to be consistent if the same numerical values for $C_m, C_a, C_{ma}=-C_{am}$ can be used for a description of all these different phenomena.

Appendix

A) Formulas for $\mathcal{P}^{(m)}:\overline{\boldsymbol{e}_1\boldsymbol{e}_2}$

Let γ'_m, γ''_m be real quantities with

$$\gamma'_{-m}=\gamma'_m, \quad \gamma''_{-m}=-\gamma''_m, \quad m=0,\pm 1,\pm 2.$$

Then

$$\sum_{m=-2}^{+2}(\gamma'_m+i\gamma''_m)\,\mathcal{P}^{(m)}=\gamma'_0\,\mathbf{1}+\sum_{m=1}^{2}(\gamma'_m-\gamma'_0)\,(\mathcal{P}^{(m)}+\mathcal{P}^{(-m)})+\sum_{m=1}^{2}\gamma''_m i(\mathcal{P}^{(m)}-\mathcal{P}^{(-m)})$$

applies, where $\mathbf{1}$ is a fourth rank unit tensor with $(\mathbf{1})_{\mu\nu,\mu'\nu'}=\delta_{\mu\mu'}\delta_{\nu\nu'}$. The fourth rank projection tensors $\mathcal{P}^{(m)}$ contain the unit vector $\boldsymbol{h}$ parallel to the magnetic field [11]. The expressions $\mathcal{P}^{(m)}:\overline{\boldsymbol{e}_1\boldsymbol{e}_2}$ can be evaluated by insertion of explicit formulas [11] for $\mathcal{P}^{(m)}$; $\boldsymbol{e}_1$ and $\boldsymbol{e}_2$ are arbitrary unit vectors, $\overline{\boldsymbol{e}_1\boldsymbol{e}_2}=\frac{1}{2}(\boldsymbol{e}_1\boldsymbol{e}_2+\boldsymbol{e}_2\boldsymbol{e}_1)-\frac{1}{3}\boldsymbol{e}_1\cdot\boldsymbol{e}_2\,\boldsymbol{\delta}$. The result is stated in the following form:

$$(\mathcal{P}^{(1)}+\mathcal{P}^{(-1)}):\overline{\boldsymbol{e}_1\boldsymbol{e}_2}=(\boldsymbol{h}\cdot\boldsymbol{e}_1)\,\overline{\boldsymbol{e}_2\boldsymbol{h}}+(\boldsymbol{h}\cdot\boldsymbol{e}_2)\,\overline{\boldsymbol{e}_1\boldsymbol{h}}-2(\boldsymbol{h}\cdot\boldsymbol{e}_1)(\boldsymbol{h}\cdot\boldsymbol{e}_2)\,\overline{\boldsymbol{h}\boldsymbol{h}},$$

$$(\mathcal{P}^{(2)}+\mathcal{P}^{(-2)}):\overline{\boldsymbol{e}_1\boldsymbol{e}_2}=\overline{\boldsymbol{e}_1\boldsymbol{e}_2}+\tfrac{1}{2}\overline{\boldsymbol{h}\boldsymbol{h}}\,[(\boldsymbol{h}\cdot\boldsymbol{e}_1)(\boldsymbol{h}\cdot\boldsymbol{e}_2)+\boldsymbol{e}_1\cdot\boldsymbol{e}_2]-(\boldsymbol{h}\cdot\boldsymbol{e}_1)\,\overline{\boldsymbol{e}_2\boldsymbol{h}}-(\boldsymbol{h}\cdot\boldsymbol{e}_2)\,\overline{\boldsymbol{e}_1\boldsymbol{h}},$$

$$i(\mathcal{P}^{(1)}-\mathcal{P}^{(-1)}):\overline{\boldsymbol{e}_1\boldsymbol{e}_2}=(\boldsymbol{h}\cdot\boldsymbol{e}_1)\,\overline{\boldsymbol{h}\,\boldsymbol{h}\times\boldsymbol{e}_2}+(\boldsymbol{h}\cdot\boldsymbol{e}_2)\,\overline{\boldsymbol{h}\,\boldsymbol{h}\times\boldsymbol{e}_1},$$

$$i(\mathcal{P}^{(2)}-\mathcal{P}^{(-2)}):\overline{\boldsymbol{e}_1\boldsymbol{e}_2}=\tfrac{1}{2}\overline{\boldsymbol{e}_1\,\boldsymbol{h}\times\boldsymbol{e}_2}+\tfrac{1}{2}\overline{\boldsymbol{e}_2\,\boldsymbol{h}\times\boldsymbol{e}_1}-\tfrac{1}{2}(\boldsymbol{h}\cdot\boldsymbol{e}_1)\,\overline{\boldsymbol{h}\,\boldsymbol{h}\times\boldsymbol{e}_2}-\tfrac{1}{2}(\boldsymbol{h}\cdot\boldsymbol{e}_2)\,\overline{\boldsymbol{h}\,\boldsymbol{h}\times\boldsymbol{e}_1}.$$

B) The Gas-Flow Wheatstone Bridge

For the determination of the "longitudinal" viscosity coefficients (i. e. of η_1, η_2, η_3) the capillary C_1 is part of a gas-flow Wheatstone bridge [1, 2, 4]. In the setup used in Ref. [4] C_1 is placed in a magnetic field, the three other capillaries C_2, C_3, C_4 are outside the magnet. Without any field (this is indicated by the superscript ^{0}) the bridge is in equilibrium, i. e. there is no pressure difference between points a and b (which are connected by a manometer):

$$p_a{}^0=p_b{}^0. \tag{B 1}$$

In the presence of a field the pressure difference p_a-p_b is measured. If J_i and R_i denote the mass flow and the flow resistance in capillary C_i ($i=1,\dots,4$) the following relations apply:

$$J_1=\frac{p_A-p_a}{R_1}, \quad J_2=\frac{p_a-p_B}{R_2}, \quad J_3=\frac{p_A-p_b}{R_3}, \quad J_4=\frac{p_b-p_B}{R_4}. \tag{B 2}$$

Since there is no gas flow through the manometer (i. e. between points a and b) we have

$$J_1=J_2, \quad J_3=J_4. \tag{B 3}$$

Through the action of a magnetic field the mass flow through capillary C_1 changes and an additional pressure difference $\Delta p_1=p_A-p_a-(p_A{}^0-p_a{}^0)$ occurs. By the use of Eqs. (B 1) – (B 3) the relation

$$J_1-J_1{}^0=-\delta J_1{}^0\Delta p_1/(p_A{}^0-p_a{}^0) \tag{B 4}$$

is established. Here δ assumes the values 0, ε, ∞ according to which of the quantities J_1, $p_A - p_B$ or $p_A - p_a$ is kept constant when the magnetic field is switched on:

$$\delta = \begin{matrix} 0 \\ \varepsilon \\ \infty \end{matrix} \quad \text{for} \quad \begin{matrix} J_1 = J_1^0 , \\ p_A - p_B = p_A^0 - p_B^0 , \\ \Delta p_1 = 0 . \end{matrix} \tag{B 5}$$

For an ideal bridge the factor

$$\varepsilon = \frac{R_1^0}{R_2^0} = \frac{R_3^0}{R_4^0} = \frac{p_A^0 - p_a^0}{p_a^0 - p_B^0} \tag{B 6}$$

is equal to 1.

The pressure difference Δp_1 is proportional to the measured quantity $p_a - p_b$:

$$-\frac{(1+\varepsilon)^2}{\varepsilon} \frac{p_a - p_b}{p_A - p_B} = 1 - \frac{R_1^0}{R_1} = (1+\delta) \frac{\Delta p_1}{p_A^0 - p_a^0} . \tag{B 7}$$

Hence, also

$$\frac{J_1 - J_1^0}{J_1^0} = \frac{\delta}{1+\delta} \frac{(1+\varepsilon)^2}{\varepsilon} \frac{p_a - p_b}{p_A - p_B} \tag{B 8}$$

applies. In particular, Eq. (B 7) shows that $(1+\delta) \Delta p_1$ is independent of δ.

Since the flow resistance is proportional to viscosity, i. e. $R_1^0 \propto \eta$, $R_1 \propto \eta_{\text{eff}}$, we have for small changes $\Delta \eta = \eta_{\text{eff}} - \eta$

$$1 - R_1^0 / R_1 = \Delta \eta / \eta . \tag{B 9}$$

Then, the comparison of (B 7) with (B 9) yields a relation between $\Delta \eta$ and $p_a - p_b$ or Δp_1:

$$\frac{\Delta \eta}{\eta} = (1+\delta) \frac{\Delta p_1}{p_A^0 - p_a^0} = -\frac{(1+\varepsilon)^2}{\varepsilon} \frac{p_a - p_b}{p_A - p_B} . \tag{B 10}$$

Acknowledgements

Thanks are due to Prof. Dr. L. Waldmann, Priv. Doz. Dr. S. Hess, and to Dr. H. Hulsman for many helpful discussions.

[1] For a review see e. g. J. J. M. Beenakker and F. R. McCourt, Ann. Rev. Phys. Chem. **21**, 47 [1970].
[2] J. Korving, Physica **50**, 27 [1970].
[3] H. Hulsman, E. J. van Waasdijk, A. L. J. Burgmans, H. F. P. Knaap, and J. J. M. Beenakker, Physica **50**, 53 [1970].
[4] H. Hulsman, F. G. van Kuik, K. W. Walstra, H. F. P. Knaap, and J. J. M. Beenakker, Physica **57**, 501 [1972].
[5] L. J. F. Hermans, J. M. Koks, A. F. Hengeveld, and H. F. P. Knaap, Physica **50**, 410 [1970]. — J. P. J. Heemskerk, L. J. F. Hermans, G. F. Bulsing, and H. F. P. Knaap, Physica **57**, 381 [1972].
[6] H. Vestner, Thesis "Transporterscheinungen und Randbedingungen in mehratomigen Gasen im Magnetfeld", Erlangen 1973.
[7] H. Vestner, Z. Naturforsch. **28 a**, 869 [1973].
[8] L. Waldmann, Z. Naturforsch. **12 a**, 660 [1957]; **13 a**, 609 [1958]. — R. F. Snider, J. Chem. Phys. **32**, 1051 [1960].
[9] F. R. McCourt and R. F. Snider, J. Chem. Phys. **46**, 2387 [1967]; **47**, 4117 [1967].
[10] S. Hess and L. Waldmann, Z. Naturforsch. **21 a**, 1529 [1966]; **23 a**, 1893 [1968]. — H. H. Raum and W. E. Köhler, Z. Naturforsch. **25 a**, 1178 [1970].
[11] S. Hess and L. Waldmann, Z. Naturforsch. **26 a**, 1057 [1971].
[12] H. Vestner, Z. Naturforsch. **28 a**, 1554 [1973].
[13] L. Waldmann, Z. Naturforsch. **22 a**, 1269 [1967].
[14] H. Vestner, Z. Naturforsch. **29 a** [1974].
[15] J. Halbritter, Thesis "Ableitung einer Randbedingung für die Verteilungsfunktion eines Gases aus linearen rotierenden Molekülen", Erlangen 1972; Z. Naturforsch., to be published.
[16] S. Hess, Springer Tracts in Mod. Phys. **54**, 136 [1970].
[17] H. Hulsman and H. F. P. Knaap, Physica **50**, 565 [1970].
[18] F. Baas, Phys. Letters **36 A**, 107 [1971]; Physica, to be published.